



## A study of the B+B double-lined eclipsing binary u Her

Somaya Saad<sup>1\*</sup> and Mohamed Nouh<sup>1,2</sup>

<sup>1</sup> National Research Institute of Astronomy and Geophysics, Helwan, Cairo, Egypt

<sup>2</sup> Faculty of Science, Northern Border University, Arar, Saudi Arabia

Received 2010 December 03; accepted 2011 June 15

**Abstract.** Using new spectroscopic data, we re-investigate the B-type eclipsing binary u Her. The method of spectrum disentangling is used to decompose the spectrum of the system to its individual spectra. Comparison of the decomposed spectra with the theoretical spectra is done to obtain the main fundamental parameters for both components. We analyzed a total of 50 new electronic spectra obtained through 1994–2004 of the spectroscopic binary star u Her. The radial velocity variations of the binary components are analyzed. The orbital solution suggests a circular orbit with a period of  $2.^d051$  and semi amplitude of  $101 \pm 1 \text{ km s}^{-1}$ . Comparison against the synthetic grid gives  $T_{eff} = 19000 \pm 1000 \text{ K}$ ,  $\log g = 3.5 \pm 0.25$  with  $v \sin i = 145 \pm 5 \text{ km s}^{-1}$  for the primary and  $T_{eff} = 11000 \pm 250 \text{ K}$ ,  $\log g = 3.5 \pm 0.25$  with  $v \sin i = 105 \pm 5 \text{ km s}^{-1}$  for the secondary.

*Keywords* : stars: variables – binaries: eclipsing – stars: individual: u Her

### 1. Introduction

The stellar system u Her (68 Her, HR 6431, HD 156633, BD +33 2864, HIP84573), with  $m_v = 4.63$  is a well-known, short-period (2.051d) eclipsing binary in the northern hemisphere with two resolved components. Both components are B-type stars classified as B1.5+B4 (Popper 1980) and B2+B8 (Hilditch 1984). The binary system belongs to a group of short-period, early-type, semi-detached systems and is significantly different from classical Algol systems in which the secondary component is supposed to fill its Roche-lobe (e.g. Jabbar, Jabir & Fleyeh 1987), while the primary one is expected to display  $\beta$  Cephei-type variability (Hilditch 1984). Parallax measurement by Hipparcos is  $3.77 \pm 0.56 \text{ mas}$ . Photometric observations and light curve analyses have been done by Rovithis & Livaniou (1980), Jabbar et al. (1986, 1987) using optical B and V filters and by Van der Veen (1985) using a narrow band photometric system. Hilditch (2005) again reinvestigated u Her and derived new orbital and astrophysical parameters for the system.

---

\*e-mail:ssmsaad@nriag.sci.eg

Recently with a large dataset of spectroscopic observations Uytterhoeven et al. (2008) gave the first evidence for pulsation character of the primary component of the u Her binary system.

In the present work we have revised and presented some new results for u Her using new spectroscopic observations covering the long wavelength range from 4000-7500 Å obtained by the high-resolution Heidelberg Extended Range Optical Spectrograph (HEROS). We could resolve the spectra for both components mainly around He I 6678 Å and through some phases around H $\alpha$ . The radial velocities (RVs) of the secondary component could be measured as well as K2 and mass ratio for the system. In the radial velocity variations of the mean profile of H $\alpha$ , comp-1 represents a new feature which may be explained by pulsation of the primary component or variations due to mass transfer. Main physical parameters are obtained by carrying out model atmosphere analyses under LTE and NLTE assumptions and comparison with synthetic spectra. Comparison with other previous parameters are also discussed.

## 2. Observations, data reduction and analyses

### 2.1 Observations

The data available for this study consist of 50 electronic spectrograms. All spectra were obtained at the Ondrejov 2-m Telescope using three different detectors.

1. 35 Reticon spectrograms covering the wavelength region 6300-6740 Å and obtained using the coude focus with a Reticon RL-1872F/30 detector at a reciprocal dispersion of 17 Å/mm during the years 1994-2000.
2. 12 spectrograms in the wavelength region 6260-6772 Å obtained with a CCD camera attached to the coude focus between 2002 and 2004.
3. 3 spectrograms in the wavelength region 3600-8300 Å obtained at the red and blue channels of the fibre-fed echelle spectrograph HEROS attached to the Cassegrain focus between 2000 and 2004.

### 2.2 Data reduction and analysis

A complete reduction process for Reticon spectra i.e wavelength calibration, rectification and intensity were all carried out using SPEFO (SPEctroFOtometry) program developed by J. Horn (for more details see Horn et al. 1992; Skoda 1996). All initial reduction of HEROS and CCD spectra (bias subtraction, flat fielding and wavelength calibration) were carried out using modified MIDAS and IRAF packages, respectively. The resulting FITS files from the original sources were transferred to the SPEFO format where the rectification and measurements were done. All acquisition times were transferred to the heliocentric frame, and the measured RVs were shifted

to the zero-point using a set of telluric lines and the technique described by Horn, Kubat & Harmanec (1996).

Direct RV measurements were obtained interactively using the SPEFO program by means of the best fit of the direct and reverse images of the measured line profile. Through the oscilloscopic mode the enlarged spectral line is shown together with its mirrored profile (in another colour) that can be interactively shifted by ( $\Delta\lambda$ ) until the shifted wavelength and that of the laboratory wavelength match at ( $\lambda_o$ ) of the selected line. We measured radial velocities for five different components, three for H $\alpha$  and two for HeI lines. The spectra of the secondary component of u Her is clearly seen at definite phases. RV measurements using H $\alpha$  were obtained by fitting the outer broad wings of the line (comp. 1), and then by fitting the deepest part of the line, i.e. the absorption core (comp. 2); at some phases we could define the position of the secondary, so we were able to fit and measure it (comp. 3) as shown in Fig. 1. For HeI 6678 Å line, comps. (4) and (5) were obtained by fitting the primary and secondary components respectively as shown in Fig. 2. For H $\alpha$  it was not easy to achieve accurate radial velocity measurements specially for the secondary component due to its wide variability as an early type star; the orbital phases were calculated using ephemeris of Uytterhoeven et al. (2008) HJD 2450343.24+2.<sup>d</sup>0510354 E. Table 1 represents the RV measurements of u Her where columns 1, 2 and 3 refer to the file number, HJD (Heliocentric Julian Date) and HVel (Heliocentric radial velocity correction) respectively while columns 4, 5 and 6 represent the measurements of each of the three components of H $\alpha$ . Columns 7 and 8 represent the RVs for both the primary and the secondary components of HeI 6678 Å line.

### 3. Orbital solution

The orbital elements were obtained using the Hadrava code FOTEL (**F**OTometric **E**lement). FOTEL is a FORTRAN program for separate or simultaneous solutions of light and RV curves of binary and triple systems at individual zero points for each data set (Hadrava 1993; Hadrava 2004a). Measured RVs of H $\alpha$  and HeI 6678 Å for the primary and the secondary components were used to obtain solution I. FOTEL calculates the errors of the adjusted elements and their mutual correlations by means of a covariance matrix. In all cases the accepted solutions were those with minimum sum of squares of residuals. Table 2 displays the orbital solutions of u Her where Solution I is a FOTEL solution while Solutions II and III are KOREL (**K**ORrelation **E**lements) solutions (Hadrava 2009 and references therein) obtained from H $\alpha$  and HeI 6678 Å respectively.

### 4. Spectrum disentangling

For this purpose we used the code KOREL for Fourier disentangling i.e. simultaneous decomposition of component spectra and finding orbital solutions (Hadrava 1995, 1997, 2004b, 2009). We identify the secondary spectral lines and proceeded in our analysis using the good spectra. KOREL solution for HeI and H $\alpha$  are obtained for primary and secondary components. In addition, for H $\alpha$  we obtained simultaneous solutions for the binary parameters with those of the telluric ones. The secondary from H $\alpha$  and weak one of HeI were found. Fig. 3 illustrates the KOREL

**Table 1.** The measured radial velocities for different components of u Her.

File No.	HJD	HVel	H $\alpha$			HeI 6678 Å	
			Comp-1	Comp-2	Comp-3	Comp-4	Comp-5
r4625	49476.4043	8.85	20.33	-103	—	-111.8	—
r4650	49480.3904	7.87	17.37	-110	—	-114.8	—
r7876	49811.4932	14.81	-37.13	54	-164.2	80.72	-156.9
r8052	49841.3448	8.96	-3.28	-108	82.42	-120.1	101.4
r8054	49841.3879	8.93	10.81	-114	91.12	-121.8	99.13
r8061	49841.4347	8.88	10.19	-118	100.25	-123.4	153.4
r8065	49841.555	8.68	11.21	-117	106.27	-121.6	151.6
r8357	49898.5214	-6.79	-8.68	-61	95.61	-94.51	—
r8493	49909.515	-9.48	-30.87	-38.5	—	-19.91	—
r10765	50232.5407	1.79	-10.92	26	—	25.82	—
r11104	50278.4018	10.15	0.18	-110	98.38	-116	175.3
r11148	50281.4067	10.82	-46.28	61	-176.7	78.56	-214.4
r11553	50318.4783	16.31	-57.80	42	-215.8	58.5	-175.9
r11563	50319.3152	16.21	1.048	-106	115.61	-117.1	151.3
r11568	50319.4368	16.36	-2.565	-94	76.83	-112.8	179.6
r13337	51076.3356	16.34	1.860	-107	116.71	-102.1	192.3
r13548	51238.6438	16.92	-33.55	-28.28	—	-37.86	—
r13626	51250.5685	16.84	17.32	-115	150.9	-123.6	194.3
r13787	51315.5194	5.37	-20.52	24.5	—	39.5	—
r13882	51325.5085	2.63	-43.48	56.6	-226.1	71.47	-202.6
r13912	51327.5457	2	-42.11	58.5	-231.7	71.14	-203.6
r14179	51385.3856	-12.44	-23.06	-30.7	—	-36.81	106.8
r14268	51391.375	-13.49	-27.71	19.2	—	42.42	—
r14517	51413.4106	-16.21	-20.6	51.96	-99.01	70.05	-156.3
r14634	51421.4005	-16.64	-12.79	-2.3	—	-0.436	—
r14673	51427.3857	-16.76	-17.15	9.73	—	-28.55	—
r15834	51626.5702	16.08	-7.54	45	57.43	43.3	57.1
r16005	51661.4846	10.3	-15.17	41	—	51.23	-133.3
r16056	51667.4675	8.9	-20.58	-65	52.06	-18.75	86.98
r16130	51672.4874	7.61	-16.15	-16.73	—	-13.25	—
r16199	51681.4483	5.3	-0.1	-92	—	-103.5	—
r16300	51698.4778	0.5	-29.37	46.7	-179.8	60.3	-170.1
r16341	51699.4616	0.25	2.806	-75.6	80.65	-95.01	145.4
r16467	51708.5125	-2.38	-19.54	-18	—	-5.33	—
la28074	52303.6609	14.04	-33.05	69.5	-203.0	88.88	-120.8
la28077	52303.6784	14.03	-48.31	72	-207.7	88.85	-212.5
lb20075	52308.6649	14.82	0.44	-73	89.56	-99.02	111.5
mg20019	52841.3937	-11.48	-33.38	23.9	-211.7	74.92	-149.8
mi20017	52903.3467	-16.32	-30.5	-61	36.09	-93	115.6
mi20018	52903.3516	-16.32	-29.92	-60	38.43	-91.85	98.26
mi20019	52903.3577	-16.33	-27	-59.2	29.59	-93.02	81.5
mi20020	52903.3644	-16.33	-27.88	-59	31.22	-92.16	74.62
mi20021	52903.3715	-16.33	-24.66	-64	33.99	-97.64	94.3
mi21020	52904.2926	-16.21	-33.16	0.25	—	-10.4	—
ne19023	53145.4017	4.53	-5.24	-72.1	68.82	-79.78	76.01
ne19024	53145.4071	4.52	-8.2	-70	69.19	-81.53	58.48
rbn4019	52427.5127	0.86	—	—	—	-93.14	—
rbn4105	52440.5032	-2.78	-17.5	-28	—	-94	—
rbn5931	52727.5305	15.57	-11.7	-64.2	110.63	-98.62	87

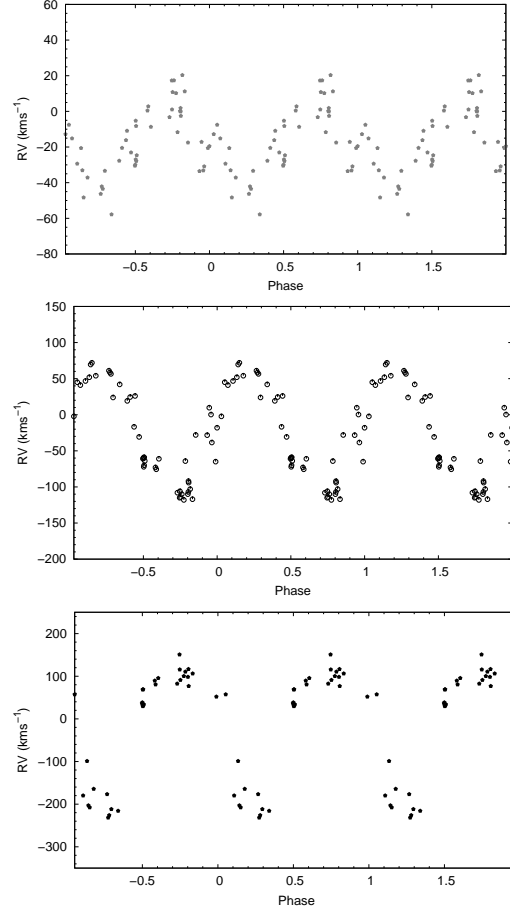


**Figure 1.** The measured RVs for  $H\alpha$ ; the top, middle and bottom panels represent the phase diagrams of components 1, 2 and 3 respectively as discussed in the text.

decomposed profiles, and the corresponding radial velocity curves of the binary system u Her obtained from  $H\alpha$ .

## 5. Analysis of stellar atmosphere

Our analysis relies on a mixing grid of NLTE and LTE synthetic spectra. For NLTE, we have adopted the grid of model spectra of early B-type stars calculated by Hubeny & Lanz (2007). The grid is computed for the temperature range  $15000 \leq T_{eff} \leq 30000\text{K}$ , in steps of 1000K, surface gravity  $1.75 \leq \log g \leq 4.75$  in steps of 0.25 dex. We adopt the grid computed at turbulent velocity =  $2 \text{ km s}^{-1}$ . For LTE calculations, we adopted as input models, the ATLAS9 grids (Ku-

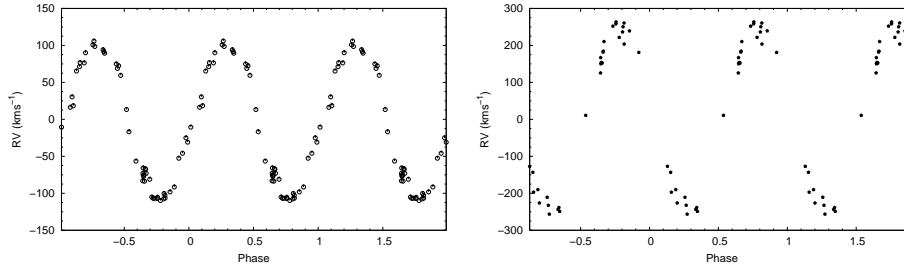


**Figure 2.** The measured RVs for He I 6678 Å; the left and right panels represent the phase diagrams of components 4 and 5 respectively

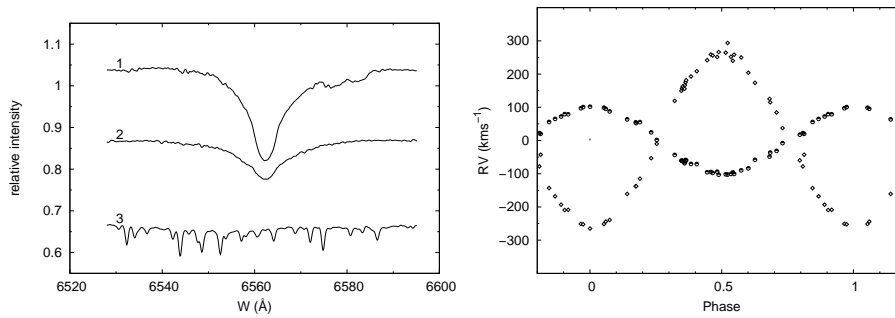


**Figure 3.** Left panel: the decomposed line profile obtained by KOREL for H $\alpha$ ; the numbers 1, 2 and 3 indicate the profiles of the primary, the secondary and the telluric lines respectively; the profiles are shifted arbitrarily for clarity. Right panel: the corresponding radial velocity curves for both components as obtained from KOREL.

ruz 1995) which consist of 409 models in total, assuming a solar metallicity, a microturbulent velocity of  $2 \text{ km s}^{-1}$  and a mixing length to scale height ratio  $L/Hp=1.25$ . Effective temperatures span the range  $3500 \leq T_{eff} \leq 14000\text{K}$ , with steps in the model grid of 250K for stars cooler than 10000K, and increasing up to 2500K for hotter stars. Surface gravity span the range  $1 \leq \log g \leq 5$ .

LTE spectra were synthesized by using the LTE stellar spectral synthesis program SPECTRUM written by Gray (1992, 1993, 1994). SPECTRUM inputs include the columns for the mass depth points, the temperatures and the total pressure, which then computes using a system of seven nonlinear equilibrium equations at each level in the atmosphere, the number densities of hydrogen, helium, carbon, oxygen and nitrogen, their relevant ions, all possible diatomic molecules that can be formed by these species and the electron number densities. The synthetic spectra were computed for the region 3000-7000 Å. We first used the  $\chi^2$  method to compare the composite observed spectra with the theoretical ones. This comparison against the synthetic grid gives  $T_{eff}=19000 \pm 1000\text{K}$ , and  $\log g=3.5 \pm 0.25$ .

**Table 2.** Orbital solutions for u Her

Element	Solution I	Solution II	Solution III
	FOTEL H $\alpha$ and He (Prim+Sec)	KOREL H $\alpha$	KOREL HeI 6678 Å
$P$ [d]	2.051044±0.00001	2.05097	2.051042
$T_{periast.}$	50344.99±0.009	50342.9237	50342.9305
$K_1$ (km s $^{-1}$ )	101±1	97.97	97.79
$K_2$ (km s $^{-1}$ )	252±1.8	265	265
$q$	0.40±0.009	0.369	0.369
$e$	0.0 ( <i>fixed</i> )	0.0	0.0
$\omega$ (deg)	0.0 ( <i>fixed</i> )	0.0	0.0
$i$ (deg)	78.59		
$\gamma(1)$ (km s $^{-1}$ )	-18.17		
$\gamma(2)$ (km s $^{-1}$ )	-20.21		
$\gamma(3)$ (km s $^{-1}$ )	-17.16		
$\gamma(4)$ (km s $^{-1}$ )	-21.85		
$\gamma(\text{mean})$ (km s $^{-1}$ )	-19.28		
$f(m)(M_{\odot})$	0.21921		
$M_1(M_{\odot})$	6.8		
$M_2(M_{\odot})$	2.8		
$A \sin i(R_{\odot})$	14.01		
No. of RVs/spectra	194	48	49
rms (km s $^{-1}$ )	22		

Using the code ROTIN3 we calculated grid of rotational spectra for  $100 \text{ km s}^{-1} \leq v \sin i \leq 200 \text{ km s}^{-1}$  in steps of  $5 \text{ km s}^{-1}$ . Then we applied the  $\chi^2$  criterion to determine the best rotational velocity. To do this, we used the spectral line MgII 4481 Å in the fitting process. The determined projected rotational velocity is calculated as  $v \sin i = 145 \pm 5 \text{ km s}^{-1}$ . The observed spectra as well as the fitted model are plotted in Fig. 4. As seen in the figure, the helium lines, which are a fundamental tool to determine both the effective temperatures and surface gravities of B-type stars, matches well with the synthetic spectra. The atmospheric parameters are in a good agreement with earlier spectral classification of the composite spectrum of B3 (Roman 1956), B1.5 (Lesh 1968), B2.5 (Olson 1968) and B2 (Hill et al. 1975 and Hilditch 2005).

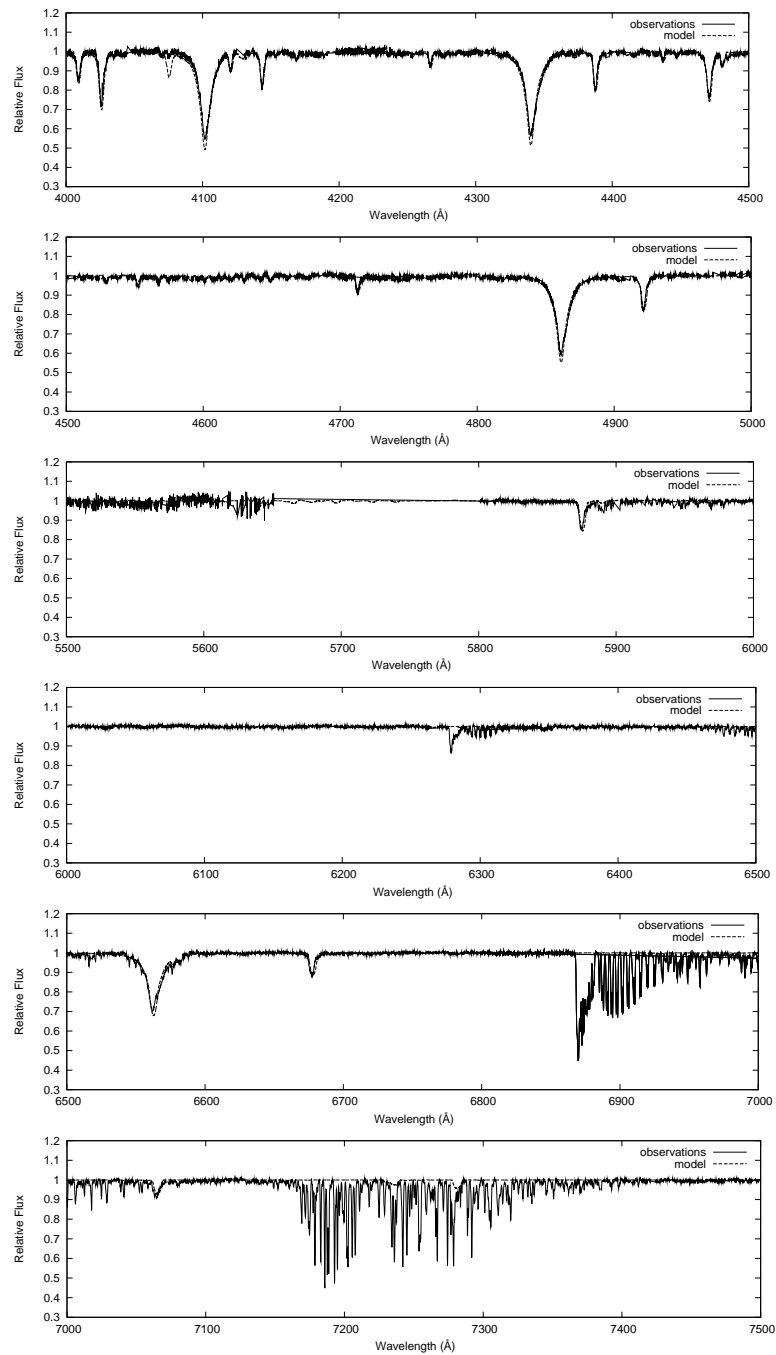


**Figure 4.** Comparison between the observed spectra of u Her and synthetic NLTE model of  $T_{eff}=19000\text{K}$ ,  $\log g=3.5$  and  $v \sin i=145 \text{ km s}^{-1}$ .

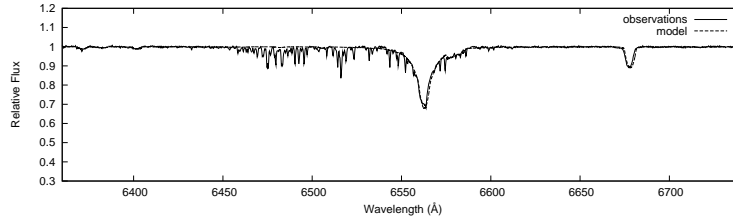


**Figure 5.** Comparison of the observed spectrum of u Her (dotted line) at phase 0.52 and the synthetic NLTE spectrum (solid line) with  $T_{eff}=19000\text{K}$ ,  $\log g=3.5$ .

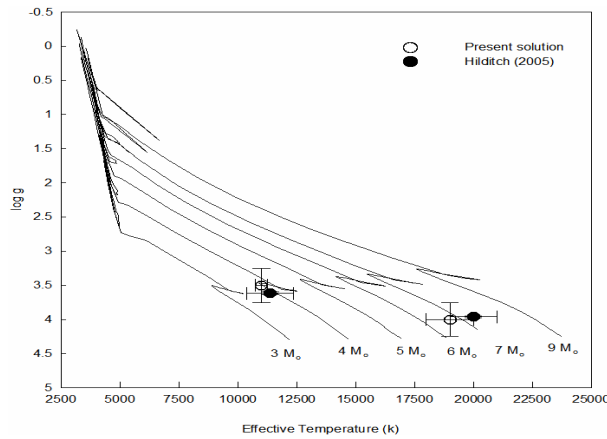


**Figure 6.** Comparison between the effective temperatures and gravities of u Her with those from the evolutionary models of Girardi et al. (2000). The positions of the two components from our solutions are plotted with open circles, while those from Hilditch (2005) are plotted with closed circles.

To determine the atmospheric parameters of the primary and secondary stars, we calculated two grids; the first with the following parameters  $19000 \leq T_{eff} \leq 23000\text{K}$ ,  $3 \leq \log g \leq 4$  and  $100 \leq v \sin i \leq 200 \text{ km s}^{-1}$  and the second grid with  $11000 \leq T_{eff} \leq 13000\text{K}$ ,  $3 \leq \log g \leq 4$  and  $100 \leq v \sin i \leq 200 \text{ km s}^{-1}$ . From a  $\chi^2$  estimate for the phase 0.52 (vastly dominated by the light of the primary star alone) we estimate  $T_{eff}=19000 \pm 1000\text{K}$ ,  $\log g=3.5 \pm 0.25$ , and  $v \sin i=145 \pm 5 \text{ km s}^{-1}$ . The effect of the residual, small fraction of light coming from the cooler secondary star is included within the formal error of the model atmosphere parameters. In Fig. 5 we plotted the spectra at phase 0.52 as well as the best fitted model. As seen in the Figure, HeI lines are fitted well, while H $\alpha$  has a reasonable fit.

The model atmospheric parameter for the primary star derived from the phase 0.52 spectrum as well as the atmospheric parameters of the composite spectra lead to the atmospheric parameters of the secondary star being  $T_{eff}=11000 \pm 250\text{K}$ ,  $\log g=3.54 \pm 0.25$  and  $v \sin i=105 \pm 5 \text{ km s}^{-1}$ .

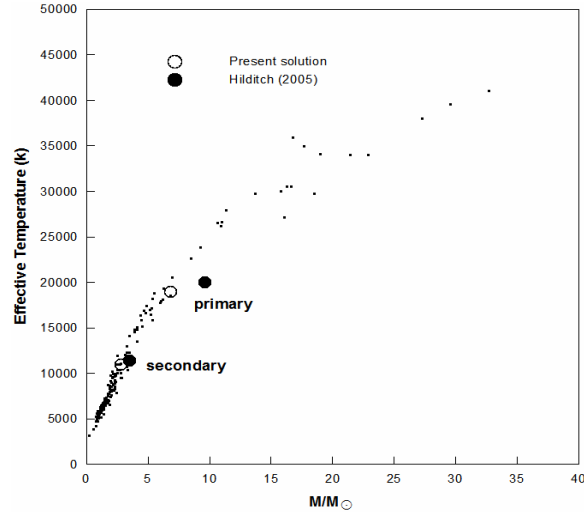


**Figure 7.** The empirical mass-effective temperature relation for intermediate mass stars by Malkov (2007). The positions of the two components from our solution are plotted with open circles, while those from the Hilditch (2005) solution are plotted with closed circles.

We compare the values derived from the present solution both with theoretical evolutionary models of Girardi et al. (2000) with metal abundance  $Z=0.019$  in Fig 6, and the mass-luminosity relation of the intermediate mass stars by Malkov (2007) in Fig 7. In the two diagrams, we have plotted our results as well as those from Hilditch (2005). One can see from Fig 6 that while the primary fits well the mass provided from the orbital solution ( $M_1=6.8M_\odot$ ), the secondary appears to have mass larger than that provided by the orbital solution ( $M_2=2.8M_\odot$ ). This differs from the result of Hilditch (2005), where the secondary fits well the mass provided from the orbital solution, but that is not the case for the primary. The mass-effective temperature relation is in good agreement with our results, while the primary component from the solution of Hilditch is less luminous for its mass by about 4000K. The difference between our result and Hilditch may be attributed to the different initial mass ratio used during the orbital calculations, while the difference on the evolutionary tracks may be due to an evolutionary model for the system taking into account the mass exchange and mass loss.

## 6. Conclusions

We have presented a new investigation for the B-type eclipsing binary u Her. Orbital solution suggests a circular orbit of  $2.^d051$  period and semi amplitude of  $101\pm 1 \text{ km s}^{-1}$ . Comparison against the synthetic grid gives  $T_{eff}=19000\pm 1000\text{K}$ ,  $\log g=3.5\pm 0.25$  and  $v\sin i=145\pm 5 \text{ km s}^{-1}$  for the primary and  $T_{eff}=11000\pm 250\text{K}$ ,  $\log g=3.54\pm 0.25$  and  $v\sin i=105\pm 5 \text{ km s}^{-1}$  for the secondary. Location of the effective temperatures and surface gravities of the components on the theoretical

evolutionary models gave masses  $M_1=6.8 M_{\odot}$  and  $M_2=2.8 M_{\odot}$  for the primary and secondary respectively which is in agreement with those obtained from FOTEL solutions.

### Acknowledgements

This research has made use of the NASA's Astrophysics Data System Abstract Service and Ondrejov observatory 2-meter Reticon spectral archive. We acknowledge the reports of both the reviewers which have helped improve the manuscript significantly. S. Saad would like to thank Dr. J. Kubat, Dr. P. Skoda, Dr. M. Slechta, Dr. M. A. Nasser and A. Shokry, and is much indebted to Prof. Dr. P. Hadrava, (author of KOREL and FOTEL codes) for his helpful discussions while using the KOREL and FOTEL codes, and for providing these codes for free.

### References

- Girardi L., Bressan A., Bertelli G., Chiosi C., 2000, *A&AS*, 141, 371  
Gray R. O., 1992, *A&A*, 265, 704  
Gray R. O., 1993, *A&A*, 273, 349  
Gray R. O., 1994, *ASPC*, 60, 75  
Hadrava P., 1993, *Contrib. Astron. Obs. Skalnaté Pleso*, 20, 23  
Hadrava P., 1995, *A&AS*, 114, 393  
Hadrava P., 1997, *A&AS*, 122, 581  
Hadrava P., 2004, *PAICz*, 92, 1  
Hadrava P., 2004, *PAICz*, 92, 15  
Hadrava P., 2009, *A&A*, 494, 399  
Hilditch R. W., 1984, *MNRAS*, 211, 943  
Hilditch R. W., 2005, *The Observatory*, 125, 72  
Hill G., Hilditch R. W., Younger F., Fisher W. A., 1975, *MemRAS*, 79, 131  
Horn J., Hubert A. M., Hubert H., Koubský P., Bailloux N., 1992, *A&A*, 259, L5  
Horn J., Kubat J., Harmanec, P., 1996, *A&A*, 309, 521  
Hubeny I., Lanz T., 2007, *ApJS*, 169, 83  
Jabbar S. R., Jabir N. L., Fleyeh H. A., Majeed O. S., 1986, *IBVS*, 2934, 1  
Jabbar S. R., Jabir N. L., Fleyeh H. A., 1987, *Ap&SS*, 135, 377  
Kurucz R. L., 1995, *Highlights of Astronomy*, 10, 407  
Lesh J. R., 1968, *ApJS*, 17, 371  
Olson E. C., 1968, *ApJ*, 153, 187  
Popper D. M., 1980, *ARA&A*, 18, 115  
Malkov O. Y., 2007, *MNRAS*, 382, 1073  
Roman N. G., 1956, *ApJ*, 123, 246  
Rovithis P., Livaniou H. R., 1980, *Ap&SS*, 70, 483  
Skoda P., 1996, in *Astronomical Data Analysis Software Systems*, *ASPC*, 101, 187  
Uytterhoeven K., Koubský P., Harmanec P., Teltng J. H., Yang S., Richards M. T. Ilyin I., 2008, *Multiple Stars Across the H-R Diagram*, *ESO Astrophysics Symposia*, Springer-Verlag, Berlin Heidelberg, p. 53  
Van der Veen W. E. C. J., 1985, *A&A*, 145, 380